RESEARCH PAPER

Effect of hollow microneedle geometry structure on mechanical stability and microfluidic flow for transdermal drug delivery applications

Gowthami Anbazhagan[1] · Sreeja Balakrishnapillai Suseela[1] · Radha Sankararajan[1]

Abstract

Hollow microneedles (MN) have been used for the past 20 years and exhibit controlled painless delivery of a wide range of drugs into the skin. Design and simulation analysis is needed before moving forward with microneedle production for successful penetration. In this study, we introduce a novel hollow microneedle array with integrated reservoir and cylindrical center lumen for transdermal drug delivery (TDD) applications. A conical and pyramidal geometry structure of hollow microneedle array was designed, with varying needle height (400–1000 μm), base diameter (150–300 μm), and tip diameter (10–30 μm). These microneedles are positioned in a 4×4 matrix array of 16 microneedles with center-to-center spacing of 650 μm. The numerical analysis is carried out with polyvinyl alcohol (PVA) as structure material using the COMSOL Multiphysics tool. A 4×4 conical and pyramidal hollow microneedle array is subjected to a stress study under axial and bending loading conditions. The effect of variation in the geometry parameter of the microneedle in relation to mechanical strength was investigated. The microfluidic analysis was performed with water and glucose as fluids with different viscosities. It has been found that the pyramidal microneedle array has a flow rate of 230 μL/min, whereas a sharper conical tip has stronger mechanical stability with less bending and has a higher flow rate of 320 μL/min.

Keywords Microneedle geometry · Polyvinyl alcohol · Structural analysis · Microfluidic analysis · Transdermal drug delivery

1 Introduction

The most common conventional ways to administer the drug into the human body are typically by oral delivery or by use of syringes and hypodermic needles. All these traditional methods are used for the past 150 years, but it has some drawbacks and limitations (Sawon and Samad 2021). Oral drug administration might cause gastrointestinal problems and pave the way for major health issues. Most syringes and hypodermic needles are painful and contagious, and pose serious health hazards (Henry et al. 1998a; Henry et al. 1998b). These needles harm the nerve endings by penetrating deeper into the dermis layer of the skin. All these limitations are eliminated by the transdermal route of drug delivery with reduced adverse effects and improved patient compliance.

Transdermal drug delivery (TDD) is regarded as a minimally invasive, patient-friendly method for drug and vaccine delivery into the skin for subsequent distribution. Generally, transdermal drug delivery systems are classified as active and passive systems, in which most of the passive devices used chemical enhancers, emulsions, and peptides as the method for skin permeation (Prausnitz 2004; Schuetz et al. 2005; Ogiso et al. 1995). In literature, some of the most popular active methods mentioned are electroporation, ultrasound, jet injectors, electroporation, microneedles, powder injection, ablation, and iontophoresis (Banga et al. 1999; Byl 1995).

✉ Gowthami Anbazhagan
gowthamia@ssn.edu.in

Sreeja Balakrishnapillai Suseela
sreejabs@ssn.edu.in

Radha Sankararajan
radhas@ssn.edu.in

1 Department of Electronics and Communication Engineering, Sri Sivasubramaniya Nadar College of Engineering, Kalavakkam, Tamilnadu 603110, India

To overcome the limitations of conventional methods, many research studies considered microneedles as one of the promising options for painless drug delivery when compared to other active devices. Microneedles (MN) are micron size needles of less than 1 mm in length especially used for efficient transdermal drug delivery (Mccrudden et al. 2013; Ita 2015). Microneedles are classified into five unique types, such as solid, coated, hollow, dissolving, and hydrogel. Based on their characteristics, each type of microneedle has merits and demerits and is specifically created with consideration for particular functions and objectives. Solid microneedle pierces the stratum corneum layer of the skin, introduces the drug into the created microchannels, and enables the drug to diffuse into the pores. Although it offers the benefit of minimizing hazardous infection, the efficiency of drug delivery is quite low. The coated microneedle is developed with the water-soluble drug coated at the tip of the solid microneedle array. When inserted into the skin, coated MN disperses with the interstitial fluid (ISF) and distributes the drug into the skin. The delivery of a very small fixed amount of drug is a benefit, but the residual microneedle tips are hazardous, since they can spread an infection to other persons. Dissolving microneedles are made from polymeric composition, upon insertion, the larger doses of the drug dissolve and diffuse into the skin. It takes time to dissolve the drug and requires specialized knowledge for manufacture (Aldawood et al. 2021). Hydrogel or swellable microneedle arrays are prepared from the aqueous blends of polymers with hydrophilic structure. It swells and consumes interstitial fluid when inserted into the skin and creates channels for the drug passage into the skin. Hollow microneedle is fabricated with the empty cavity at the center of each needle and holes at the tip. The hollow microneedle can accommodate a large dosage or volume of drug solution inside the hollow cavity. A hollow microneedle has the capacity to deliver the higher molecular weight drugs into the epidermis or upper dermis layer. The ability to inject a controlled large amount of doses makes hollow microneedles superior than the variety of "solid" microneedles that are now available. The hollow microneedles deliver drug or vaccine into the skin in an automated manner, thus overcoming the drawbacks of hypodermic needle (Waghule et al. 2019; Jung and Jin 2021).

The design of the microneedle is an important foremost factor for the needle strength to have enough penetration into the epidermis of the skin without any failure. Several researchers have reported the impact of geometry parameters on mechanical strength and flow of drug delivery. Few examples, Gittard et al. investigated the impact of microneedle geometry on skin penetration. It was mentioned that the variation in length, base diameter, and aspect ratio has direct influence on the mechanical stability of microneedle (Gittard et al. 2013). The increase in spacing between the microneedles results in efficient penetration is observed by Kochhar et al. (2013). Loizidou et al. demonstrated that variations in the base of the geometry structures with different vertices, such as square, triangular, and hexagonal base, had a great impact on structural and penetration characteristics. A conical-shaped microneedle of different vertices is used for the study. It is observed that the mechanical strength of microneedle is better in geometry with more vertices, but there is an opposite effect on transdermal permeation (Loizidou et al. 2016). In another work, three different microneedle arrays were used for the investigation on transport of fluid into the skin by Suzanne et al. The diameter and sharpness of the microneedle has direct influence on the drug delivery and transdermal vaccination (Bal et al. 2010). Recently, Ryan Donnelly and his team constructed seven different geometry structures by the alteration in basic conical and pyramidal shape for the analysis of drug delivery. The full shape conical structure has better insertion capability at low force and the design with more number of arrays has effective drug loading. The sharp and smooth edges of the microneedle contribute to efficient skin insertion and the increase in insertion force leads to higher amount of drug delivery (Cordeiro 2020).

The choice of material is an another significant aspect to achieve the mechanical stability of the microneedle (Aldawood et al. 2021). First, microneedle was developed using silicon material, and later, several research groups employed silicon to fabricate microneedles. However, it is evident that silicon is brittle and the fabrication process of silicon microneedles is quite expensive (Li et al. 2019; Pradeep Narayanan and Raghavan 2017). When a silicon microneedle breaks during penetration and there is a possibility of small silicon particles remains in the tissue. This can lead to skin damage, and sometimes, it causes serious health hazards (Sharma 2018). In most cases, metal microneedles have enough strength for skin penetration, but they are not biocompatible (Hu et al. 2020; Vinayakumar et al. 2016). However, numerous studies utilized polymer materials to fabricate microneedles with sufficient mechanical strength. The main reason of research towards the development of microneedle using polymer materials is because of its biocompatible and biodegradable nature, and also, they are reasonably priced (Gera and Burra 2022). Some biocompatible polymer materials are polycarbonate, Poly methyl methacrylate, polydimethylsiloxane, polyglycolic acid, polyvinyl alcohol, carboxymethylcellulose, etc. (Ahmed Saeed AL-Japairai 2020). The existing research works more concentrated on the modeling and analysis of single microneedle with silicon and metallic materials (Amin and Ahmed 2013). There is always a limitation in existing TDD devices with the material biocompatibility and needle stability. As a result, there is a growing demand for the creation of microneedle arrays made of biocompatible material that

is strong enough to pierce the skin and deliver drugs in a proportionate and continuous manner.

The finite-element analysis (FEA) has received a great deal of interest recently in the MN sector (Yan et al. 2022). The analysis helps to avoid expensive experimental trials and provides the pathway to create customized MN according to patient skin. All the previous works of hollow microneedle are analyzed with single microneedle of different geometry with single- or double-side opened lumen or centered lumen (Griss and Stemme 2002; Wang et al. 2009; Ranamukhaarachchi et al. 2016). Hollow SU-8 microneedles were created by Mishra et al. in a straightforward and effective manner (Mishra et al. 2018). The cylindrical body of a microneedle with a sharp tip was sufficient to puncture skin quickly and effectively. Kanakaraj et al. (Sawon and Samad 2021) introduced an out-of-plane microneedle with six lumens for drug passage. COMSOL software was used to perform the structural analysis on silicon carbide material. The work investigates the fluidic analysis utilizing various viscosity-based fluids and examines the structural mechanics of the microneedle. In another study, an investigation of the stress and flow analysis of cylindrical microneedles with a side-open lumen is performed. The experiment used PGA (polyglycolide as structural material (Bodhale et al. 2010). The microneedles are constructed with copper and silver material and ANSYS software is used to analyze the stress effect and deformation on the single microneedle (Tariq 2022).

The purpose of the work is to incorporate the hollow microneedle patch in a semi-automatic continuous glucose monitoring and insulin delivery system. The conventional insulin delivery system has limitations in automatic accurate dose of drug delivery, painless administration, and in avoiding immedicable complications. There is a demand in developing painless automatic drug delivery system for diabetes management. A semi-automatic insulin delivery system with hollow microneedle arrays, micropump, microsensors, reservoir, and transmitter and receiver section need to be developed. The key function of this miniature system is its capability to automatically provide the appropriate dosages which depends on patient's physiological data and avoids unnecessary complications.

In this research, a patch with hollow microneedle array is proposed for a controlled drug delivery device. A two-step cost-effective micromolding fabrication process is suggested for hollow microneedle array. Finally, the detailed finite-element analysis such as stress and fluidic analysis of biocompatible hollow microneedle for transdermal drug delivery is studied. A conical and pyramidal hollow microneedle array with centered open holes is proposed to confirm drug distribution after skin insertion. A built-in drug reservoir is also included in the present design and is located on the back of the microneedle array. The microneedle array is constructed

with polyvinyl alcohol (PVA), a semi-crystalline, water-soluble polymer as the structural material. We used PVA for its advantages, such as high biocompatibility, water solubility, low toxicity, and excellent physical properties. The biodegradable polymer is also hydrophilic in nature, which results in the fast diffusion of drugs and has promising applications in drug delivery systems (Oh et al. 2022). This is the first new attempt for the mechanical and fluidic analysis of conical and pyramidal microneedle array with PVA material. There are no studies that have been published on the hollow-centered PVA microneedle array with an integrated reservoir to forecast mechanical and fluid flow characteristics under different criteria. Certain additional factors, such as pressure, fluid velocity, and flow rate, must be considered while designing the microneedle for drug administration (Mcallister et al. 2000). The size and position of the lumen also plays a crucial role to get the desired flow rate (Bodhale et al. 2010). The present study elaborately discusses on the effect of geometry parameters in relation to stress and flow analysis. The geometry structure is also dependent on the flow rate of the drug; here, the conical and pyramid geometry has taken for the fluid flow analysis using different viscous fluids are investigated. This simulation is useful for analyzing the behaviour of the microneedle array, refining its design and enhancing the system performance.

2 Proposed design and fabrication process of hollow microneedle

In the proposed drug delivery system (DDS), hollow microneedle is one of the major component for controlled and efficient drug delivery. Here, the two models of hollow microneedle array are developed: 1. 4×4 conical MN array; 2. 4×4 pyramidal MN array. In this section, we designed hollow tip open microneedles with an integrated small micro-reservoir for drug storage. The three-dimensional design structure of the conical and pyramidal microneedle array is shown in Fig. 1a, b. The extensive benefit of conical and pyramidal geometric shape is that both are tapered structure which will deliver the required amount of drug to
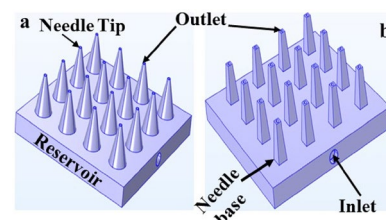

Fig. 1 Schematic illustration of proposed three-dimensional model in top view: **a** conical microneedle array and **b** pyramidal microneedle array with reservoir

the patient skin with stronger stability throughout the phase (Garcia et al. 2017). The designed microneedle has circular and square tip with hollow-centered single-lumen cylindrical body.

The microneedle array consists of 16 microneedles, placed in a 4×4 array, as shown in Fig. 1. It includes reservoir at the bottom of the microneedle array. Each microneedle has a hollow lumen that serves as an outlet, and an input inlet is constructed on one side of the microneedle patch. The micropump draws fluid from the reservoir, which enters the microneedle array through its inlet and leaves through its hollow lumen outlet. The hollow microneedle patch attached to the forearm of the patient delivers controlled fluid into the human skin. As the geometrical dimensions of the microneedle are crucial for effective penetration into the skin, the characteristics like needle-to-needle spacing, height, base diameter, and tip diameter are carefully chosen (Kochhar et al. 2013). The proposed out-of-plane conical and pyramidal microneedle is 600 μm in length, with a base diameter of 200 μm and a tip diameter of 30 μm. In this design, a centered hollow cylindrical lumen of diameter 25 μm is placed inside the conical and pyramidal needle.

Hollow microneedle arrays with centered lumens have been manufactured using a two-step micromolding procedure. The method has numerous benefits, such as simple mechanical process, easy replication, and less time consumption. This method also makes it possible to fabricate all other kinds of polymer microneedle patches. Aluminium and acrylic substrates can be used as substrates for the fabrication process. The process flow of out-of-plane hollow microneedle array is shown in Fig. 2. The acrylic mold is developed using CO_2 laser with the proper tuning of speed and power parameters. Two forms of mold, such as bottom and top mold, is developed and connected to each other with an adjustable spacing gap. Then, the process begins with the casting of polymer material on the mold and it is kept under certain temperature depends on the type of polymer solution. The polyethylene (PE) tubes are used for the drug flow in the closed-loop drug delivery system.

3 Analysis of microneedle

The cross-sectional view of single conical and pyramidal microneedle presented here is displayed in Fig. 3a, b and it is considered for the structural analysis and microfluidic analysis. H represents the microneedle length, where D_L is the diameter of the hollow cylindrical lumen, L denotes the length of hollow lumen, D_{tip} is the outer diameter of microneedle tip, and D_{base} is the base diameter of microneedle.
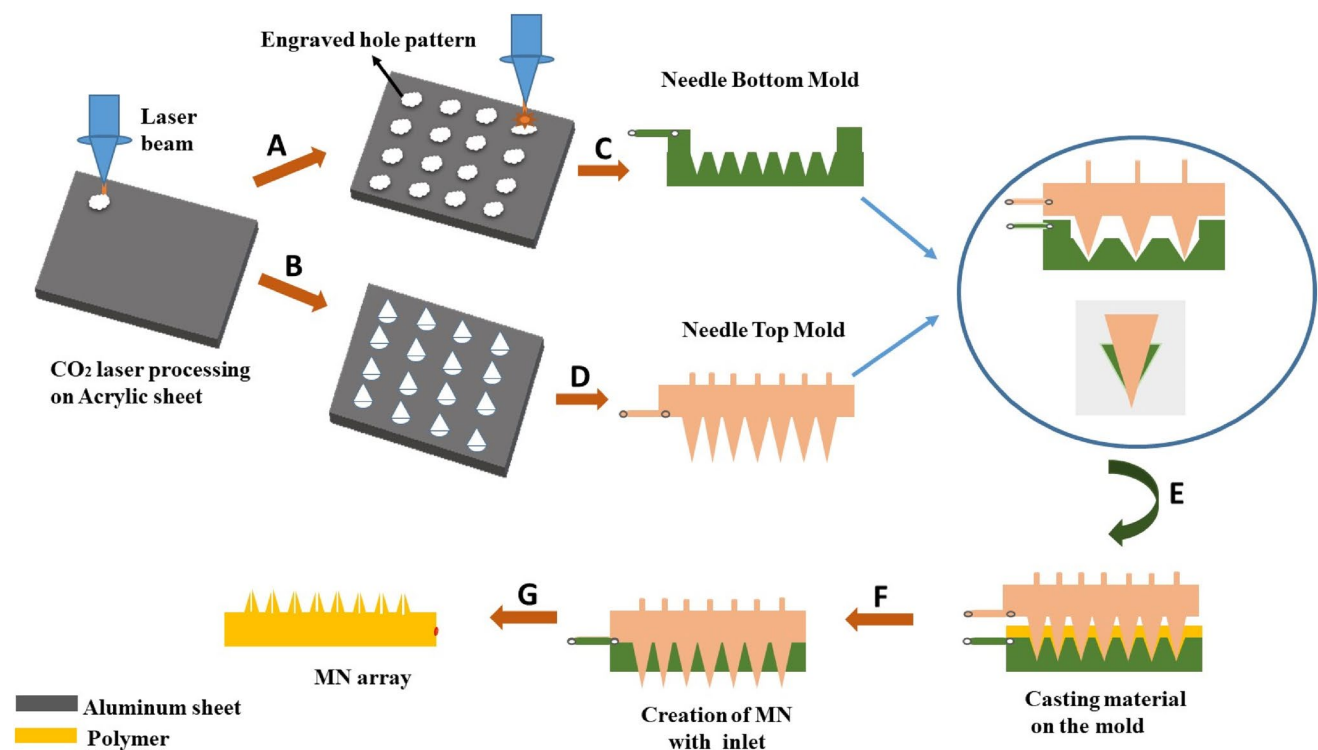

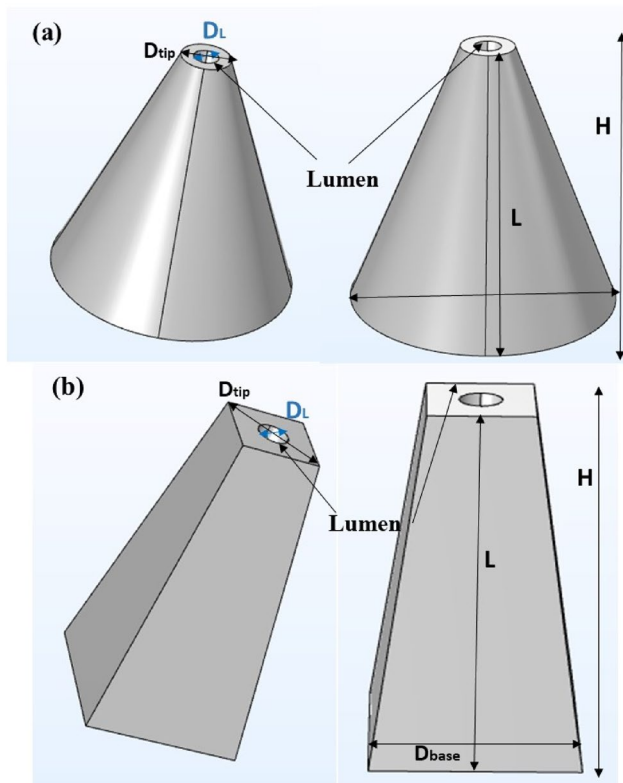**Fig. 2** Proposed fabrication flow for hollow microneedle array

Fig. 3 Cross-sectional view of **a** conical shape and **b** pyramidal shape

3.1 Structural mechanics

The microneedle will fail during skin insertion because of buckling or bending effect. The microneedle tip experiences an axial force while being inserted. The microneedle buckles due to the compressive nature of this axial force. This can be avoided by development of microneedle with smaller tip area. A sharp tapered microneedle tip minimizes buckling and skin insertion (Tayyaba et al. 2013). The skin exerts a resistive force during the insertion of the microneedle; hence, to penetrate the skin, more axial force must be supplied than the skin resistance force. However, bending can also be brought on by an uneven skin surface or a mistake made by the patient during inserting the skin. Therefore, to achieve effective microneedle design and anticipate microneedle failure, it is essential to develop a relationship between microneedle geometry and the mechanical properties of the material.

3.1.1 Axial force

The axial force that the microneedle can endure without breaking is determined by

$$F_{axial} = \sigma_y A, \tag{1}$$

where σ_y is the yield strength of the material and A is the cross-sectional area of the microneedle tip and can be stated as (Bouwstra and Ponec 2006)

$$A = \pi R^2, \tag{2}$$

where R is the radius of the microneedle tip.

3.1.2 Buckling force

The buckling force exerted on the hollow microneedle during insertion is given by (Bodhale et al. 2010)

$$F_{buckling} = \frac{\pi^2 EI}{H^2}, \tag{3}$$

where E is young's modulus of the material, I is the moment of inertia of the conical or pyramidal section, and H is the length of the microneedle.

Moment of inertia (I) for the conical section is $I = \frac{DH^3}{396}$ and moment of inertia for pyramidal section is $I = \frac{1}{12}\left(D_o^4 - D_i^4\right)$, where D_o is the outer diameter and D_i is the inner of the hollow pyramidal section (Bodhale et al. 2010).

To penetrate the human skin with a microneedle, an external force or pressure must be stronger than the skin's resistance.

3.1.3 Resistive force

The following equation identifies the skin's resistive force before a skin puncture

$$F_{resistance} = P_{pierce} A, \tag{4}$$

where P_{pierce} is the required pressure to pierce the microneedle into the skin. The needle always penetrates into the skin at a particular angle. A microneedle fracture or break during skin puncture is a serious risk.

3.1.4 Bending force

The bending force at which the microneedle can withstand without breaking is determined by

$$F_{bending} = \frac{\sigma_y I}{cH}, \tag{5}$$

where $c = \frac{D_{base}}{2}$ is the distance from the vertical axis to the outer edge of the section (Aggarwal and Johnston 2004).

3.2 Microfluidic mechanics

To understand the behaviour of fluid flow within hollow lumen microneedles, microfluidic analysis is very essential. In the case of hollow microneedle, the drug is transported more effectively through the lumen. The microneedle array experiences pressure drop during fluid flow for a variety of reasons, including microneedle shape, array size, fluid viscosity, surface roughness, and microneedle density. There is a significant amount of resistance acting on the microneedle, while fluid is passing through it. Measurements and forecasts of fluid mechanics are essential when developing microneedles for transdermal drug delivery, so that the microneedles are painless, easily pierce the skin, and large enough to attain the appropriate flow velocity (Tayyaba et al. 2013).

Poiseuille's law is employed to determine the fluid flow through the microneedle array for the cylindrical lumen

$$Q = \frac{\pi D_l{}^4 (\Delta P)}{128 \mu H}, \tag{6}$$

where Q is the flow rate, D_l is the inner diameter of the hollow lumen, ΔP denotes pressure variation across the microneedle lumen, H denotes the length of the microneedle, and μ is the fluid viscosity.

We may consider an extended Bernoulli equation to model the microneedle geometry as given by

$$\frac{P_{\text{inlet}}}{\rho g} + \frac{V_i}{2g} + Z_1 = \frac{P_{\text{outlet}}}{pg} + \frac{V_o}{2g} + Z_2 + \frac{fl}{d} + \frac{V^2}{2g} + \sum \frac{KV^2}{2g}, \tag{7}$$

where P_{inlet} is inlet pressure, P_{outlet} is outlet pressure, V_i is inlet fluid velocity, V_o is outlet fluid velocity, f is friction factor, ρ denotes the density of the fluid, and K is considered as loss coefficient factor due to inlet and outlets. The output pressure, velocity, and distances (Z_1 and Z_2) stay constant, because the cylindrical portion is symmetrical about a vertical axis.

The Reynolds number specifies the type of flow, which is expressed as

$$R_e = \frac{\rho dV}{\mu}. \tag{8}$$

If R_e is less than 2100, flow is regarded as laminar; otherwise, it is considered to be turbulent.

The friction factor for laminar fluid flow is calculated by

$$f = \frac{64}{R_e}. \tag{9}$$

The pressure drop through the microneedles can be calculated from Eq. (6)

$$\Delta P = \mu \frac{128 Q H}{\pi D_l{}^4} + \rho \frac{8 Q^2}{\pi^2 D_l{}^2} (K_1 + K_2), \tag{10}$$

where K_1 and K_2 are the loss coefficient factors due to circular and square edge inlet and outlet.

4 Numerical simulation

Two distinct types of simulations have been performed on a microneedle array using COMSOL Multiphysics 5.6, to determine the appropriate microneedle design for drug delivery. The conical and pyramidal structure of the 4×4 hollow microneedle array was designed for structural analysis to examine the mechanical characteristics of the microneedle. The fluid flow rate of 4×4 hollow microneedle array was examined using microfluidic analysis.

4.1 Mechanical analysis

The structural or mechanical analysis of the 4×4 microneedle array was analyzed with COMSOL Multiphysics. During skin penetration, the microneedle is subjected to several stresses, including bending and axial forces (Aswani Kumar et al. 2021). For axial and bending stress analysis, the array of out-of-plane microneedles was modeled with a fixed base and a free tip end. A variety of suitable geometry structures and material types were used to construct the structural model. A polymer material such as polyvinyl alcohol (PVA) was considered for analysis with Young's modulus of 707.9 MPa, Poisson ratio of 0.4, density of 1190 kg/m³, and molar mass of 86.09 g/mol. PVA has a fracture strength of 48.4 MPa, which was taken into account during structural analysis (Jain et al. 2017).

The axial stress analysis was carried out by applying pressure in the z-direction at the tip of the microneedle. The human skin can be penetrated at a pressure of 3.183 MPa. This is the resistive force offered by the skin during skin puncturing (Henry et al. 1998a, 1998b). When the microneedle is inserted into human skin, the pressure is applied to all 16 microneedles in an array, and the axial force predominates because of skin resistance. As the area of the tip of the microneedle shrinks, very less piercing pressure is needed (Yan et al. 2022). The tip of the proposed conical and pyramidal structure is extremely sharp, and hence, less pressure will be needed to pierce human skin than the specified piercing pressure. The performance analysis is made by applying the pressure of 3.18 MPa and the outcome is shown in Fig. 4. Figure 4a depicts the simulation outcome for the axial stress analysis of conical microneedle array and Fig. 4b for pyramidal microneedle array. Since the tip of the microneedle experienced a maximum stress of 3.02 MPa (conical), which is less than the yield strength of
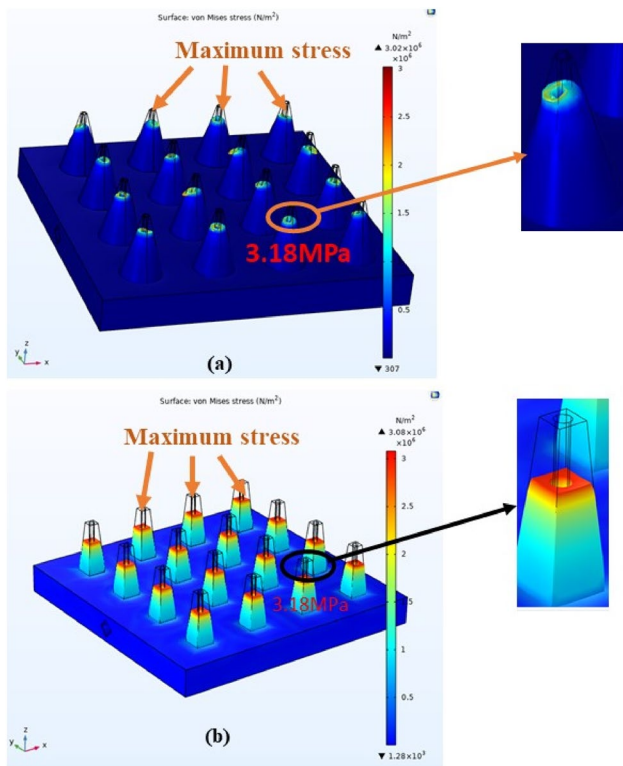
Fig. 4 Axial stress analysis: **a** conical MN array and **b** pyramidal MN array ($H = 600$ μm, $D_{base} = 200$ μm, $D_{tip} = 30$ μm)

material, the proposed microneedle can successfully pierce the skin. The simulation output of the axial stress analysis also demonstrates very little tip deflection because of applied pressure at the tip of conical and pyramidal structures. The microneedle can therefore be used gently for transdermal drug administration applications, because it will not break under the applied axial load of 3.16 MPa in the Z-direction.

In this simulation, the geometrical structures were subjected to transverse loads to perform bending stress analysis. The transverse force ranged from 0.1 to 2 mN is applied to the microneedle tip along the *x*-axis (Shibata et al. 2007). Equation (4) provides the value for transverse force based on the fracture strength of the material. The simulation output from the current study demonstrates the impact of bending stresses on the microneedle tip and lumen section during skin penetration. Both of the designs of PVA-based microneedles have been subjected to analysis. Figure 6 shows the simulation result for the applied bending force of 0.1788 N at the tip. The simulation analysis depicted in Fig. 5 revealed that the maximum stress occurs at the microneedle array for the applied bending force, which is less than the yield stress of the material.

The numerical analysis carried out in this work indicates that the lumen area or the bottom of the microneedle will not be affected by the applied loading at the tip of the microneedle. The outcome allows for the prediction that the proposed microneedle design would successfully pierce human skin. The present simulation analysis also assisted to choose
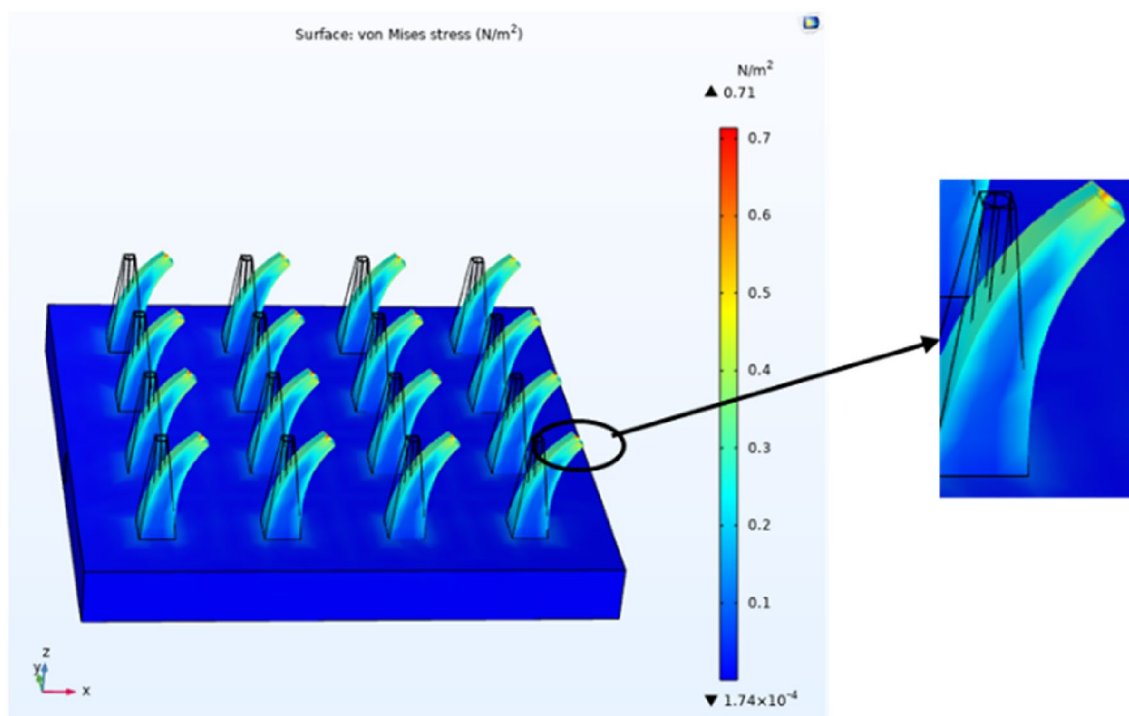

Fig. 5 Bending stress analysis of 4×4 pyramidal microneedle array ($H = 600$ μm, $D_{base} = 200$ μm, $D_{tip} = 30$ μm)

appropriate polymeric material such as polyvinyl alcohol (PVA) for microneedle fabrication.

4.2 Microfluidic analysis

In this simulation, a microfluidic analysis also called computational fluid dynamic (CFD) study was investigated to calculate pressure, velocity, and fluid flow rate through microneedle array. The inlet of the microneedle array was subjected to a pressure ranging from 10 to 100 kPa, because these ranges are suggested for various micro-pumping devices (Sawon and Samad 2021). Water and glucose were considered as working fluids in the fluid domain. Table 1 lists the characteristics of the fluids employed in the simulation investigation. The outlet pressure was assumed to be zero (Khumpuang et al. 2003). The pressure distribution through a 4×4 microneedle array at an applied pressure of 100 kPa is shown in Fig. 6a, b. The simulation output demonstrates that pressure and fluid flow distribution are uniform along the microneedle array. The microneedle array needs a consistent pressure distribution to administer the

Table 1 Properties of fluids for microfluidic analysis

Fluids	Density (kg/m^3)	Dynamic viscosity (Pa·s)
Water	997	0.00089
Glucose	1088	0.00209

drug in the correct dosage. The maximum fluid pressure of 1.01e^5 (conical) and 0.9e^5 (pyramidal) has been observed through each microneedle. Figure 7 depicts the velocity profile in microfluidic analysis at 100 kPa applied pressure.

In microfluidic analysis, the maximum fluid velocity was witnessed through each microneedle. The fluid distribution is uniform in all 16 microneedles which can be observed in Fig. 7b, d. The velocity of the fluid directly depends on factors, such as fluid density, viscosity, and area of the lumen. As the designed lumen area is very smaller, the velocity of the fluid increases inside the hollow lumen. The fluid velocity is lesser at the wall area when compared to the lumen core region due to frictional losses.

5 Results and discussion

5.1 Stress analysis

The mechanical strength of the microneedle is analyzed in detail using structural mechanics physics in COMSOL and the microneedle strength is investigated by stress analysis and occurrence of deformation. By the use of Eq. (1), the maximum compressive force is calculated as 41.76 mN. Theoretically, the skin resistive force is computed and determined to be 0.3 μN. The obtained maximum bending force was 0.1788 N (pyramidal) and 0.087 N (conical). The FEA simulation in Fig. 5 demonstrated that the highest level of stress occurred at a tip section after applying the mathematically anticipated bending force at the tip of the microneedle.
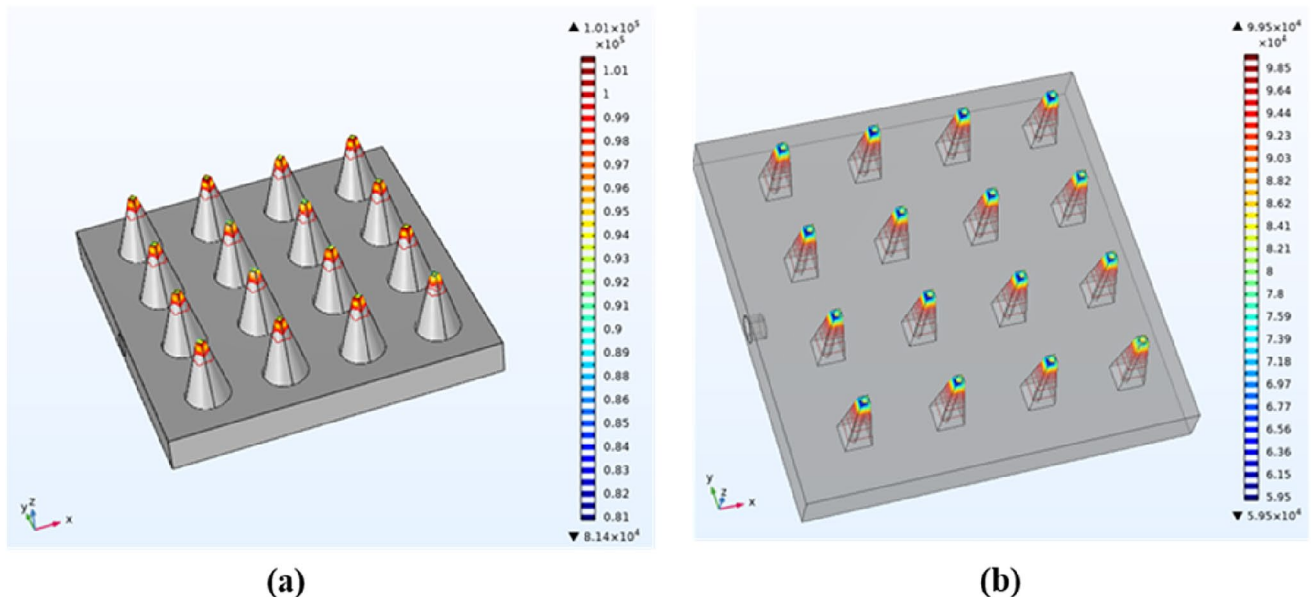

Fig. 6 Pressure distribution for 4×4 microneedles' array with water as fluid for **a** conical microneedle array and **b** pyramidal microneedle array ($H = 600$ μm, $D_{base} = 200$ μm, $D_{tip} = 30$ μm)
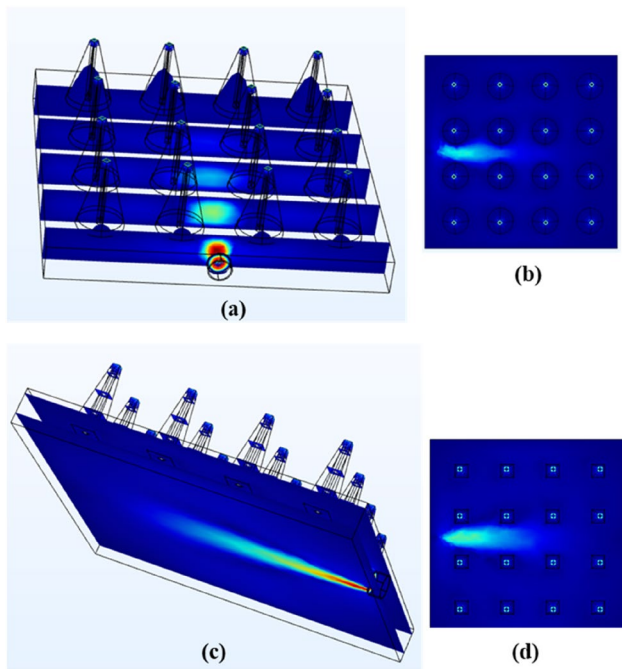
Fig. 7 Velocity profile across the plane in CFD analysis. **a** 3D view of a conical MN array with uniform velocity distribution. **b** Top view of the velocity distribution of fluid in conical microneedle array. **c** 3D view of velocity distribution in pyramidal microneedle array. **d** Top view of velocity profile with the prominent fluid flow across pyramidal microneedle array ($H = 600$ µm, $D_{base} = 200$ µm, $D_{tip} = 30$ µm)

Furthermore, a microneedle has significant difficulties in reducing pain at the time of insertion. The most significant parameter to control this problem is the geometry of the microneedle. The parameters, such as needle shape, needle length, base, and tip diameter and needle interspacing, were directly dependent on the stress acting on the microneedle array (Gill et al. 2008). In this work, the effect of geometry on the mechanical strength of the microneedle is analyzed with the investigation of the following dimensions, *Microneedle length*: 450, 600, 800, and 1000 µm; *Microneedle tip diameter*: 10, 20, 25, and 30 µm; and *microneedle base width*: 150, 200, 250, and 300 µm.

The simulation was performed by applying axial and bending loading on the different conical and pyramidal structures. The needle height directly relates to the mechanical stability of the microneedle and the depth of penetration of the microneedle into the skin. As the length of the microneedle increases from 450 to 1000 µm, the stress at the tip of the microneedle also increases and results in an increased chance of instability. The axial loading is applied at the tip of the microneedle; therefore, the maximum stress is generated at the tip surface and the smallest stress is dispersed to the needle body. Figure 8a shows the von Mises stress variation due to a change in microneedle length. The surface area of the circular shape tip for a conical microneedle is more when

compared to a square shape tip for a pyramidal microneedle. Therefore, the circular-shaped conical microneedle will undergo more stress during axial loading and experiences less bending in the tip of the conical structure. The conical geometry has a sharper structure and easily penetrates into the skin without any bending or failure, as shown in Fig. 8b. The uneven surfaces or human errors during insertion may lead to bending of needle.

The base diameter of the microneedle is investigated with the variation from 150 to 300 µm; the increase in the bottom base of the microneedle will result in minimum stress and deflections and enhance the stability of the structure with increased penetration percentage. Both the structures undergo more stress variations depicted in Fig. 8c, d.

The variation in tip surface generates stress differences on the skin due to different pressure distributions on the microneedle tip. Figure 8e shows the variation in stress brought on by changing the microneedle tip diameter under an axial load with constant boundary conditions. During axial loading, stress rises with the increase of the tip surface and an optimal stress of 4 MPa is obtained at a tip diameter of 30 µm. Then, the stress drops quickly as the tip surface increases. The larger needle tip radius induces more pain at the injection site (Ita 2015). From the FEA analysis shown in Fig. 8f, it is evident that a conical structure with a circular tip has less bending and strong enough, so that it does not break when inserted inside the skin.

Another aspect that affects the stress distribution during penetration is displacement. A microneedle with a high displacement can cause a significant amount of pain, harm skin tissues, and accidentally break itself (Shu et al. 2021). The measurement of displacement caused by altering the microneedle geometry is depicted in Fig. 9a–c. Figure 9a shows that displacement gradually increases with microneedle length. Figure 9b validates that less deformation in the conical microneedle array compared to the pyramidal structure, and in Fig. 9c, it is noted that the displacement increases as the base of the microneedle structure increases. The microneedle array with a tip diameter of 30 µm produces more displacement. Hence, a lesser tip surface results in smooth penetration into the human skin without breakage. From the above results, the miniaturized sharp tapered conical microneedle array has obtained better stability than the pyramidal geometry with less stress and displacement value. The proposed 4×4 conical microneedle array can withstand bending and axial forces which results in less discomfort and less skin irritation and tissue damage.

5.2 Flow analysis

The fluidic analysis is conducted with an applied input pressure in the 10–100 kPa range, and the outlet pressure is assumed to be 0 kPa due to the insignificant pressure at
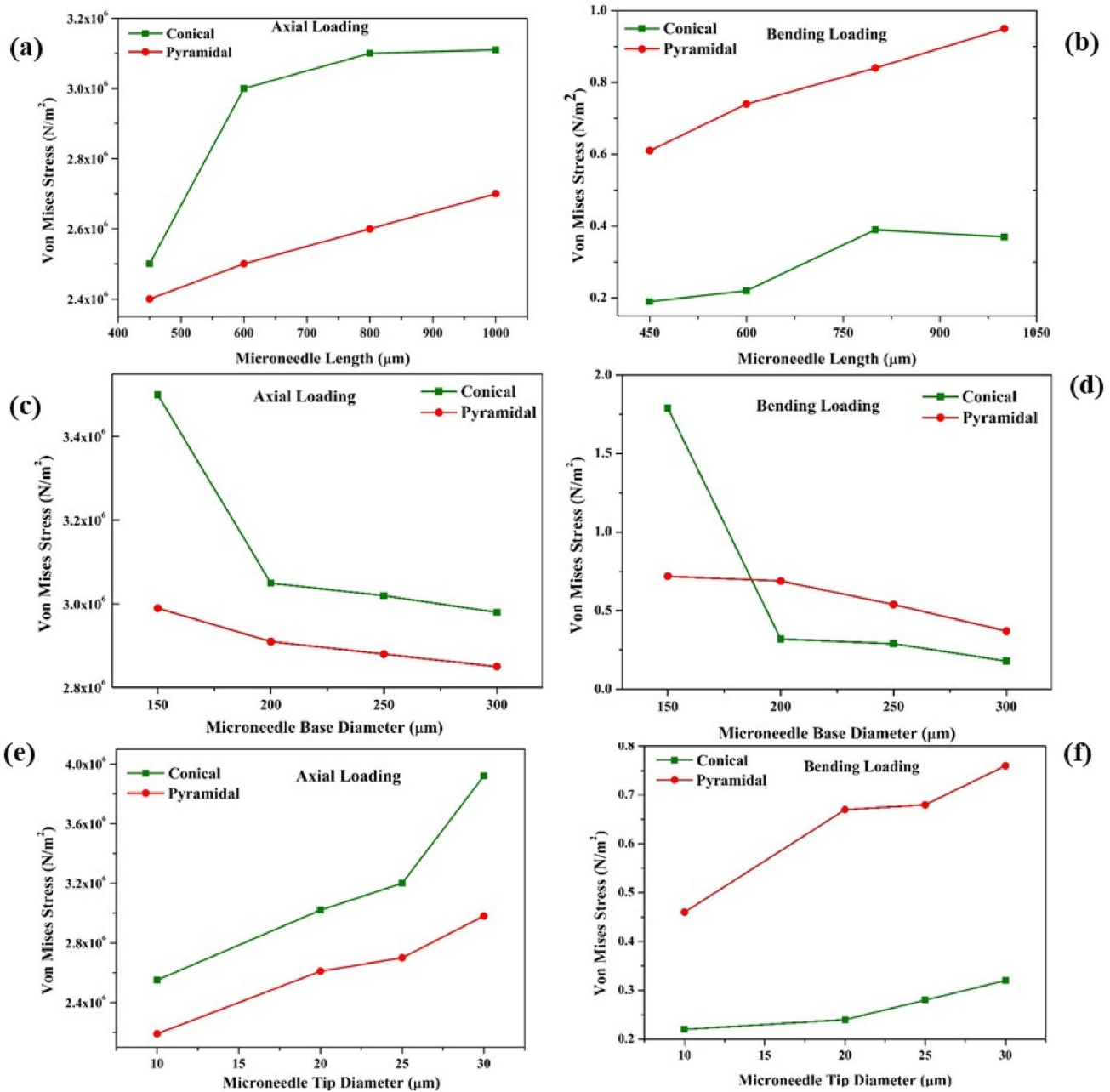
Fig. 8 Von Mises stress results for 4×4 conical and pyramidal microneedle. **a** Variation of stress with length after axial loading, **b** variation of stress with length after bending loading, **c** variation of stress with base diameter after axial loading, **d** variation of stress with base diameter after bending loading, **e** variation of stress with tip diameter after axial loading, and **f** variation of stress with tip diameter after bending loading

the outlet of the microneedle. The above-mentioned simulation results illustrate the uniform distribution of the velocity and pressure inside the microneedle. The streamlined fluid distribution inside the 4×4 conical microneedle array at an inlet pressure of 100 Kpa is displayed in Fig. 10. According to the proposed design, the pressure is initially consistent throughout the reservoir. Due to the reduction in an area towards the conical/pyramidal section,

a pressure drop takes place in the lumen section. The fluid is eventually moved towards all the holes in the microneedle array, as depicted in Fig. 7b, d. The fluid exits out from the vertical lumen at modest velocity. The depiction is similar to the flow of water from the tap, when the tap is open, pressure is high at the inlet, and the water gets splashed eventually.
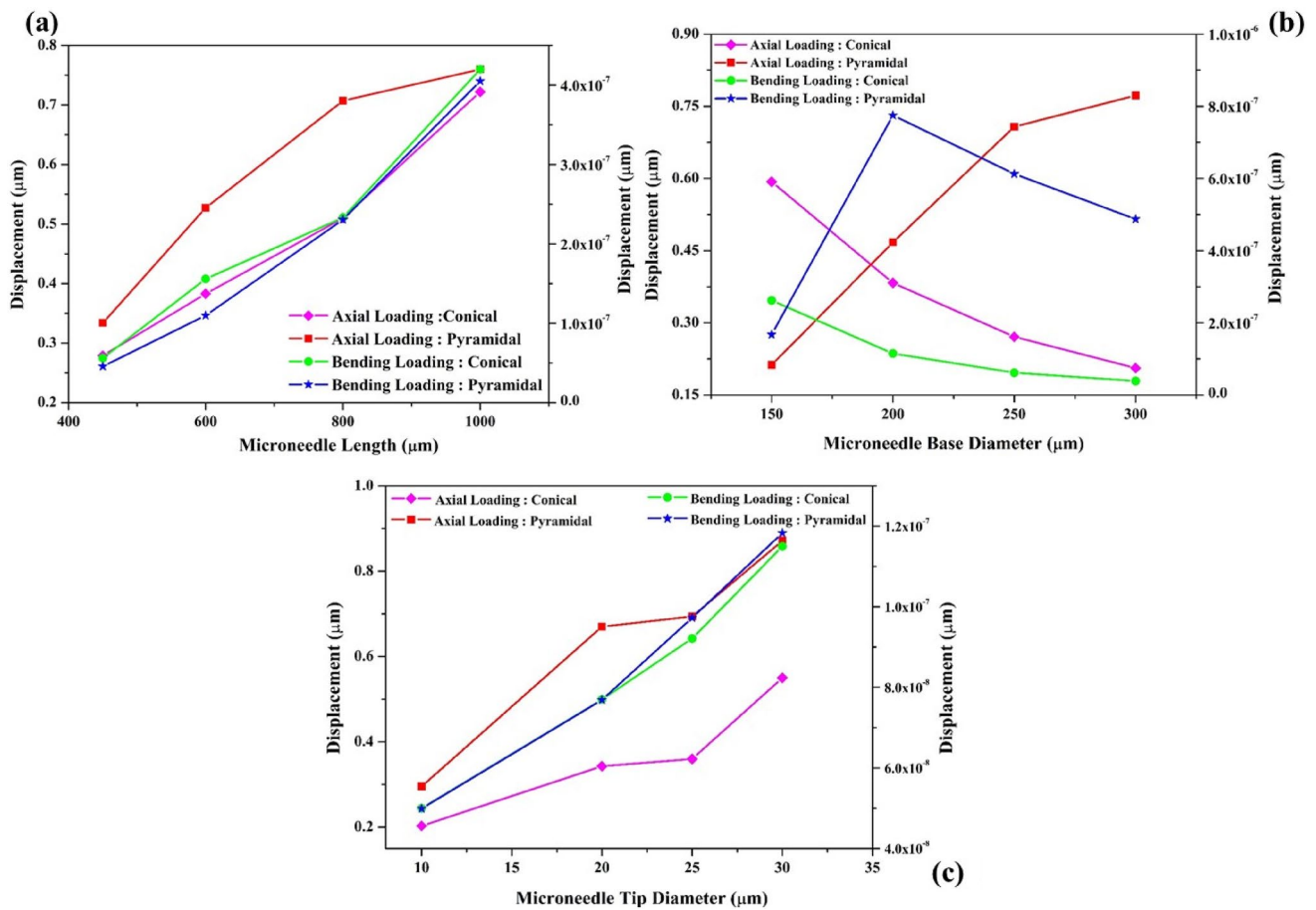
Fig. 9 Variation of displacement under axial and bending loading: **a** length, **b** base diameter, and **c** tip diameter
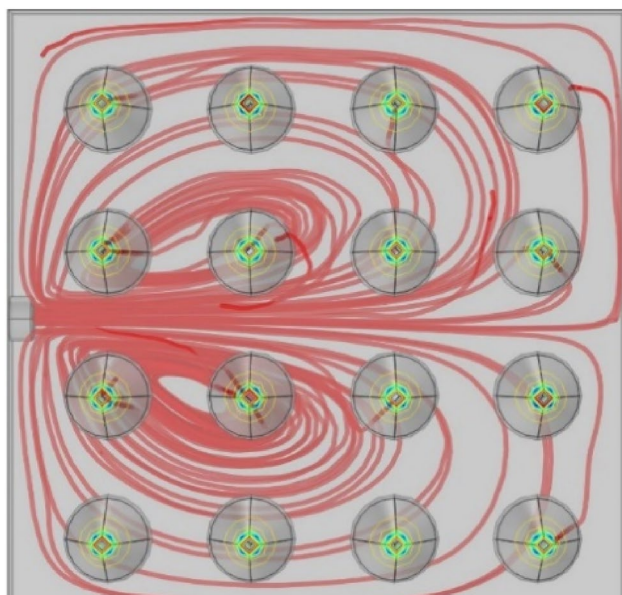

Fig. 10 Top view of streamline distribution of water fluid at a pressure of 100 KPa

Moreover, it can be inferred from the simulation that the velocity changes with fluid viscosity. Figure 11 depicts the fluid velocity curve of water and glucose with relation to change in inlet pressure. In this graph, the velocity increases with the increase of inlet pressure. Furthermore, it is apparent from the graph that due to its viscosity and density, water has a higher velocity than glucose. It is evident that flow velocity is prominent in the conical MN array when water is the selected fluid. Figure 12 shows the comparison between the flow rates of water as a fluid with variation in applied pressure. The flow rate directly depends on the fluid viscosity, and the flow rate is high for a low viscous fluid. Here, the glucose fluid is with higher viscosity of 0.00209 Pa·s (Sawon and Samad 2021), and hence, the flow rate of the water is higher when compared to the glucose. The simulation result is shown for a 4×4 conical microneedle and pyramidal MN array with water as a fluid in Fig. 12. A higher flow rate of 320 μL/min is seen in the conical MN, whereas the pyramidal MN achieves a flow rate of 230 μL/min.
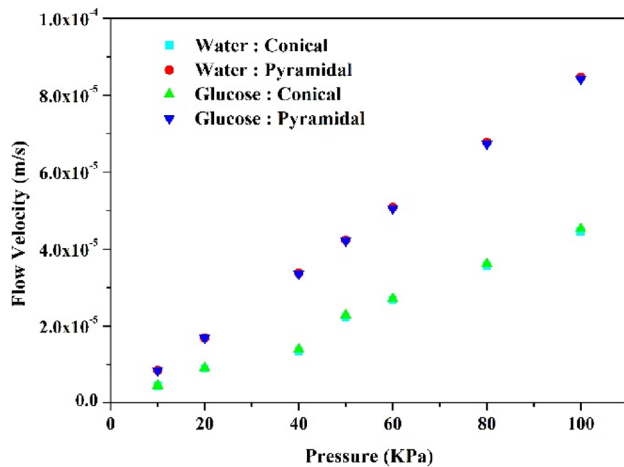
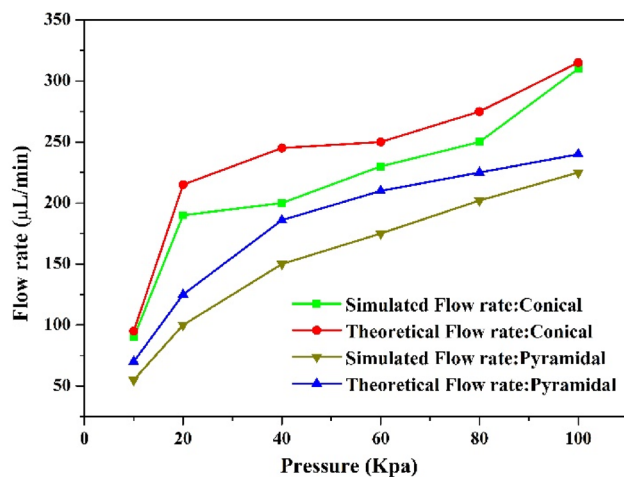**Fig. 11** Velocities of different fluids in relation to inlet pressures

Fig. 12 Comparison of theoretical and simulation flow rate of water with variation in applied pressure

6 Conclusion and future work

In this work, we presented the design of controlled drug delivery system for diabetic patients. The system is primarily developed to automatically deliver the necessary dosage of drugs in accordance with patient physiological data. The user-friendly device provides painless injection always create better patient–doctor communication. A 4×4 hollow PVA microneedle array with centered cylindrical lumen is designed and simulated for the controlled drug delivery system. The various microneedle geometry structures (conical, pyramidal) and parameters (length, base, and tip diameter) have been considered for the structural and microfluidic analysis. The following significant findings from the simulations and analysis:

1. The microneedle with different geometrical parameters is subjected to loading conditions. As observed, increasing the length of the needle increased maximum stress and has increased chance of instability. The increase in base diameter will decrease the stresses and deflections and enhancing the stability of the structure with increased penetration percentage. The microneedle with larger needle tip diameter induces more pain at injection site.

2. The biocompatible PVA MNs have enough strength to successfully pierce human flesh without breaking. The stress generated proved that the microneedle would remain intact for the applied pressure of 3.16 MPa. It was discovered that a sharp conical tip produces less tension, which leads to painless drug distribution.

3. Moreover, the fluidic analysis shows that high viscous fluid has lower velocity profile and vice versa. Similarly, the flowrate of water for conical microneedle was 320 µL/min and that for pyramidal microneedle array was 230 µL/min at 100 kPa inlet pressure.

Even though the development of hollow microneedle array is moving forward rapidly, the integration of various devices with the microneedle patch is still challenging. The future work focuses on fabrication of PVA hollow microneedle array and integration of devices with fabricated microneedle patch. In addition, we will also perform the in vivo studies with the complete prototype integrated with fabricated microneedle array on animal skin for controlled drug delivery.

Author contributions AG, BSS and SR contributed to the study concept and design. Simulation, analysis and fabrication process flow work done by AG. The result validation performed by BSS and SR. AG, BSS and SR participated in the writing and revision of the manuscript equally.

Data availability The data that support the findings of this study are available from the corresponding author upon reasonable request.

Declarations

Conflict of interest The authors declare that there is no conflict of interest.

References

Aggarwal P, Johnston CR (2004) Geometrical effects in mechanical characterizing of microneedle for biomedical applications. Sens Actuators B Chem 102(2):226–234. https://doi.org/10.1016/j.snb.2004.04.024

Ahmed Saeed AL-Japairai K et al (2020) Current trends in polymer microneedle for transdermal drug delivery. Int J Pharma 587:119673. https://doi.org/10.1016/j.ijpharm.2020.119673

Aldawood FK, Andar A, Desai S (2021) A comprehensive review of microneedles: types, materials, processes, characterizations and applications. Polymers 13(16):1–34. https://doi.org/10.3390/polym13162815

Amin F, Ahmed S (2013) Design, modeling and simulation of MEMS-based silicon microneedles. J Phys Conf Ser. https://doi.org/10.1088/1742-6596/439/1/012049

Aswani Kumar G et al (2021) Effect of insertion force for successful penetration of a conical shaped microneedle into the skin. In: Lecture notes in mechanical engineering. Springer, Singapore. https://doi.org/10.1007/978-981-15-4488-0_51

Bal SM et al (2010) Influence of microneedle shape on the transport of a fluorescent dye into human skin in vivo. J Control Release 147(2):218–224. https://doi.org/10.1016/j.jconrel.2010.07.104

Banga AK, Bose S, Ghosh TK (1999) Iontophoresis and electroporation: comparisons and contrasts. Int J Pharm 179(1):1–19. https://doi.org/10.1016/S0378-5173(98)00360-3

Bodhale DW, Nisar A, Afzulpurkar N (2010) Structural and microfluidic analysis of hollow side-open polymeric microneedles for transdermal drug delivery applications. Microfluid Nanofluid 8(3):373–392. https://doi.org/10.1007/s10404-009-0467-9

Bouwstra JA, Ponec M (2006) The skin barrier in healthy and diseased state. Biochim Biophys Acta Biomembr 1758(12):2080–2095. https://doi.org/10.1016/j.bbamem.2006.06.021

Byl NN (1995) The use of ultrasound as an enhancer for transcutaneous drug delivery: phonophoresis. Phys Ther 75(6):539–553. https://doi.org/10.1093/ptj/75.6.539

Cordeiro AS et al (2020) Two-photon polymerisation 3D printing of microneedle array templates with versatile designs: application in the development of polymeric drug delivery systems. Pharm Res. https://doi.org/10.1007/s11095-020-02887-9

Garcia J, Rios I, Fonthal F (2017) Design and analysis of microneedles structures for transdermal drug delivery. In: Proceedings of the 2016 IEEE ANDESCON, ANDESCON 2016. https://doi.org/10.1109/ANDESCON.2016.7836202

Gera AK, Burra RK (2022) The rise of polymeric microneedles: recent developments, advances, challenges, and applications with regard to transdermal drug delivery. J Funct Biomater 13(2):81. https://doi.org/10.3390/jfb13020081

Gill HS et al (2008) Effect of microneedle design on pain in human subjects. Clin J Pain 24(7):585

Gittard SD et al (2013) The effects of geometry on skin penetration and failure of polymer microneedles. J Adhes Sci Technol 27(3):227–243. https://doi.org/10.1080/01694243.2012.705101

Griss P, Stemme G (2002) Novel, side opened out-of-plane microneedles for microfluidic transdermal interfacing. In: Proceedings of the IEEE micro electro mechanical systems (MEMS), (February), pp 467–470. https://doi.org/10.1109/memsys.2002.984303

Henry S et al (1998a) Microfabricated microneedles: a novel approach to transdermal drug delivery. J Pharm Sci 87(8):922–925. https://doi.org/10.1021/js980042+

Henry S et al (1998b) Micromachined needles for the transdermal delivery of drugs. In: Proceedings of the IEEE micro electro mechanical systems (MEMS), pp 494–498. https://doi.org/10.1109/memsys.1998.659807

Hu Z et al (2020) Solid and hollow metallic glass microneedles for transdermal drug-delivery. Appl Phys Lett 116(20):203703. https://doi.org/10.1063/5.0008983

Ita K (2015) Transdermal delivery of drugs with microneedles—potential and challenges. Pharmaceutics 7(3):90–105. https://doi.org/10.3390/pharmaceutics7030090

Jain N, Singh VK, Chauhan S (2017) A review on mechanical and water absorption properties of polyvinyl alcohol based composites/films. J Mech Behav Mater 26(5–6):213–222. https://doi.org/10.1515/jmbm-2017-0027

Jung JH, Jin SG (2021) Microneedle for transdermal drug delivery: current trends and fabrication. J Pharm Investig 51:503–517. https://doi.org/10.1007/s40005-021-00512-4

Khumpuang S, Maeda R, Sugiyama S (2003) Design and fabrication of a coupled microneedle array and insertion guide array for safe penetration through skin. In: MHS 2003—proceedings of 2003 international symposium on micromechatronics and human science, vol 1, pp 233–237. https://doi.org/10.1109/MHS.2003.1249938

Kochhar JS et al (2013) Effect of microneedle geometry and supporting substrate on microneedle array penetration into skin. J Pharm Sci 102(11):4100–4108. https://doi.org/10.1002/jps.23724

Li Y et al (2019) Fabrication of sharp silicon hollow microneedles by deep-reactive ion etching towards minimally invasive diagnostics. Microsyst Nanoeng. https://doi.org/10.1038/s41378-019-0077-y

Loizidou EZ et al (2016) 'Evaluation of geometrical effects of microneedles on skin penetration by CT scan and finite element analysis. Eur J Pharm Biopharm 107:1–6. https://doi.org/10.1016/j.ejpb.2016.06.023

Mcallister DV, Allen MG, Prausnitz RM (2000) M icrofabricated M icroneedles for G ene. Molecules 2:289–313

Mccrudden MTC et al (2013) Microneedles for intradermal and transdermal delivery. Eur J Pharm Sci 50(5):623–637. https://doi.org/10.1016/j.ejps.2013.05.005.Microneedles

Mishra R, Maiti TK, Bhattacharyya TK (2018) Design and scalable fabrication of hollow SU-8 microneedles for transdermal drug delivery. IEEE Sens J IEEE 18(14):5635–5644. https://doi.org/10.1109/JSEN.2018.2840335

Ogiso T, Iwaki M, Paku T (1995) Effect of various enhancers on transdermal penetration of indomethacin and urea, and relationship between penetration parameters and enhancement factors. J Pharm Sci 84(4):482–488. https://doi.org/10.1002/jps.2600840418

Oh NG, Hwang SY, Na YH (2022) Fabrication of a PVA-based hydrogel microneedle patch. ACS Omega 7(29):25179–25185. https://doi.org/10.1021/acsomega.2c01993

Pradeep Narayanan S, Raghavan S (2017) Solid silicon microneedles for drug delivery applications. Int J Adv Manuf Technol 93(1–4):407–422. https://doi.org/10.1007/s00170-016-9698-6

Prausnitz MR (2004) Microneedles for transdermal drug delivery. Adv Drug Deliv Rev 56(5):581–587. https://doi.org/10.1016/j.addr.2003.10.023

Ranamukhaarachchi SA et al (2016) Integrated hollow microneedle-optofluidic biosensor for therapeutic drug monitoring in sub-nanoliter volumes. Sci Rep 6(July):1–10. https://doi.org/10.1038/srep29075

Sawon MA, Samad MF (2021) Design and optimization of a microneedle with skin insertion analysis for transdermal drug delivery applications. J Drug Deliv Sci Technol. https://doi.org/10.1016/j.jddst.2021.102477

Schuetz YB et al (2005) Emerging strategies for the transdermal delivery of peptide and protein drugs. Expert Opin Drug Deliv 2(3):533–548. https://doi.org/10.1517/17425247.2.3.533

Sharma D (2018) Microneedles: an approach in transdermal drug delivery: a review. Pharmatutor 6(1):07. https://doi.org/10.29161/pt.v6.i1.2018.7

Shibata T et al (2007) Fabrication and mechanical characterization of microneedle array for cell surgery. In: Transducers and EURO-SENSORS '07—4th international conference on solid-state sensors, actuators and microsystems, vol 3(September), pp 719–722. https://doi.org/10.1109/SENSOR.2007.4300231

Shu W et al (2021) Insights into the mechanics of solid conical microneedle array insertion into skin using the finite element method. Acta Biomater 135:403–413. https://doi.org/10.1016/j.actbio.2021.08.045

Tariq N et al (2022) Numerical simulation, analysis, and fabrication of MEMS-based solid Ag and Cu microneedles for biomedical applications. Math Problems Eng 2022:1–19. https://doi.org/10.1155/2022/1633183

Tayyaba S, Ashraf MW, Afzulpurkar N (2013) Design, simulation, and fabrication of microneedles and a blood filter for use in a hemofiltration system. IEEE Trans Autom Sci Eng 10(2):252–266. https://doi.org/10.1109/TASE.2012.2230166

Vinayakumar KB et al (2016) Out-of-plane cup shaped stainless steel microneedle array for drug delivery. In: 2016 IEEE 11th annual international conference on nano/micro engineered and molecular systems, NEMS 2016, pp 172–175. https://doi.org/10.1109/NEMS.2016.7758225

Waghule T et al (2019) Microneedles: a smart approach and increasing potential for transdermal drug delivery system. Biomed Pharmacother 109:1249–1258. https://doi.org/10.1016/j.biopha.2018.10.078

Wang PC et al (2009) Hollow polymer microneedle array fabricated by photolithography process combined with micromolding technique. In: Proceedings of the 31st annual international conference of the IEEE engineering in medicine and biology society: engineering the future of biomedicine, EMBC 2009, pp 7026–7029. https://doi.org/10.1109/IEMBS.2009.5333317

Yan Q et al (2022) The finite element analysis research on microneedle design strategy and transdermal drug delivery system. Pharmaceutics 14(8):1625. https://doi.org/10.3390/pharmaceutics14081625